VISCOSITY AND FLOW PROPERTIES OF THE SEITAH OLIVINE-RICH LITHOLOGY. A.J. Brown[1], R.C. Wiens[2], P. Pinet[3], K.P. Hand[4], E. Cloutis[5], J.M. Madariaga[6], J.M. Comellas[7], M. Schmidt[8], J.I. Simon[9] V. Debaille[10], C.D.K. Herd[11], A. Udry[12], J.I. Núñez[13] N. Randazzo[11]. [1]Plancius Research, MD (adrian.j.brown@nasa.gov) [2]EAPS, Purdue Univ, West Lafayette, IN [3]IRAP, Toulouse, France [4] JPL, CalTech, CA [5]Univ Winnipeg, [6]Univ of Basque Country, UPV/EHU, [7]Univ of Hawai'i, [8]Brock Univ, Ontario, [9]NASA JSC, Houston, TX, [10]Université libre de Bruxelles, Belgium, [11]Univ of Alberta, Edmonton, [12]UNLV Las Vegas, Nevada, [13]Johns Hopkins APL, MD.

Introduction: One of the most surprising findings of th e *Perseverance* rover was the discovery of olivine cumulate in the Séitah region [1]. The rover landed and traversed to the Séitah region and collected measurements at three workspaces: **Bastide**, **Brac** and **Issole** (Fig 1). Here we use the SuperCam VISIR and LIBS to investigate the properties of the lithology in situ and determine two things: 1) the olivine-clay-carbonate regional lithology is low in Al^{3+}, which allows us to eliminate the possibility of clays which are high in Al^{3+}, 2) the viscosity of the Séitah formation is extremely low, which is a reasonable explanation for the Séitah unit to both cumulate and thin-layered (Fig 1b).

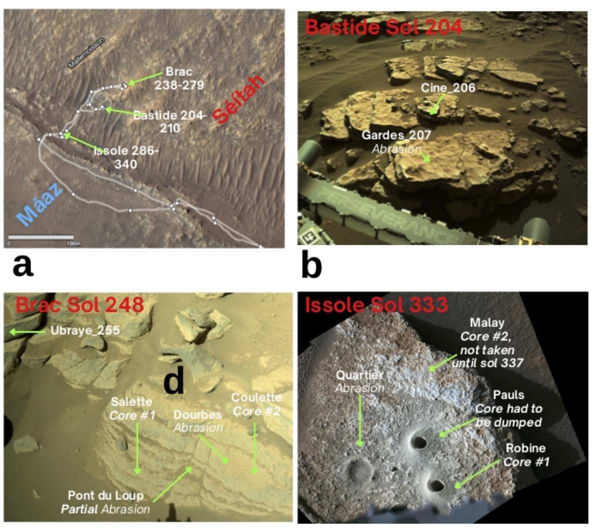

Fig. 1. Visual summary of the traverse through the Séitah formation and the three key workspaces Bastide, Brac and Issole.

SuperCam: SuperCam has been used to identify cumulate olivine and characterize its Fo# using Raman and LIBS measurements [6-7]. The SuperCam VISIR data set is being compared to spectral features seen from orbit by CRISM [3-4]. Figs 1-2 show an olivine-rich rock with a cumulate texture imaged by the SuperCam RMI and VISIR at Cine in Séitah, along with a potential terrestrial analog.

CRISM: We have utilized orbital (CRISM) data to determine the relationships between the olivine-rich lithology in the CRISM HRL40FF image.

Clay: We were able to show that clay is also present in the olivine-carbonate lithology. We have now used in situ observations to help identify the clay. We have used the SuperCam VISIR instrument onboard the rover to observe the 2-2.5 µm region of the spectrum to look for bands indicative of clays in the olivine cumulate rocks of Séitah. Using the appearance of the 2.38 and 2.46 µm bands we have been able to narrow the search to clays with metal-OH features. Finally, we have used the SuperCam LIBS instrument to determine the low (<4 wt %) Al_2O_3 thereby allowing us to eliminate clays with aluminum in their structure. The only remaining candidates are talc, lizardite, Mg/Fe smectite, hectorite, saponite and stevensite.

Viscosity: Using elemental abundances derived by the LIBS instrument on SuperCam, we have used the heuristic Giordano approach [5] to derive the viscosity of the lava flow that emplaced the Séitah cumulate [6], and find it to be exceedingly low (Figure 3a). Based on this constraint, we hypothesize that the Séitah unit was formed by a ponded flood lava from a lava flow that penetrated into Jezero crater. We further hypothesize that the Séitah olivine cumulate was formed at the base of a lava lake within Jezero crater that was part of a Nili Fossae region-wide unit.

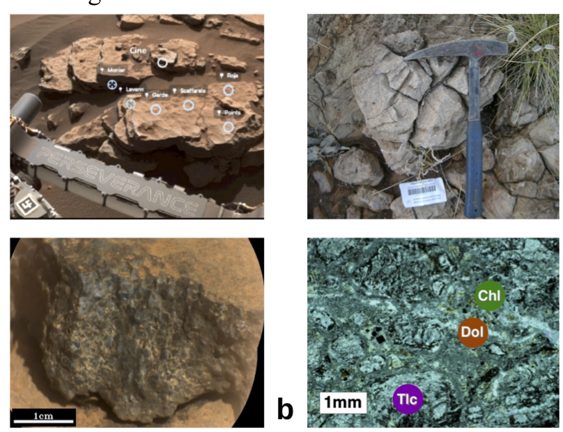

Fig. 2 (left top) Bastide workspace, location of Cine relative to Garde, rover arm for scale. (left bot) SuperCam RMI of target Cine showing olivine cumulate texture at mm scale. (right top) Context image for target AJB0503100 with hammer for scale. (right bot) Thin section of talc-carbonate sample AJB0503100 from Brown [8] with mm size talc (Tlc) replacing olivine, dolomite (Dol) and chlorite (Chl) identified using EMP. Samples from Dresser Fm, Pilbara, W.A

Flow propetries. After the calculation of the viscosity of the Séitah unit, we use the model viscosity to calculate relative flow lengths under Martian conditions using FLOWGO [8] – these results are provided in Figure 3b.

It should be noted that the Martian simulations relevant for a low pressure Mars atmosphere, as proposed in [8].

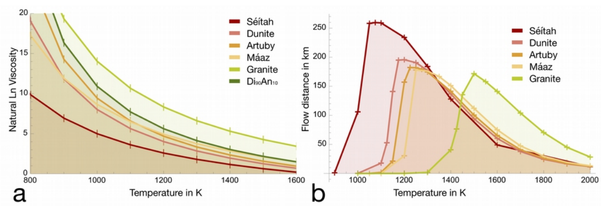

Fig 3.a. Plot of Giordano viscosity vs temp. for Máaz (orange), Séitah (red) and Artuby (marone) compared to standards. b. Relative flow lengths for viscosities of granite, dunite, Séitah, Artuby and Máaz and terrestrial analogs under Mars conditions computed using FLOWGO [8].

Convective ponded lava lake model. We used the derived viscosity to estimate the depth of the cumulate layer as around 60% of the lava pond (Figure 4) based on the model of Worster+ [9]. This involved computing the viscosity of diopside as proposed by [9] and comparing this viscosity to the viscosity of Séitah.

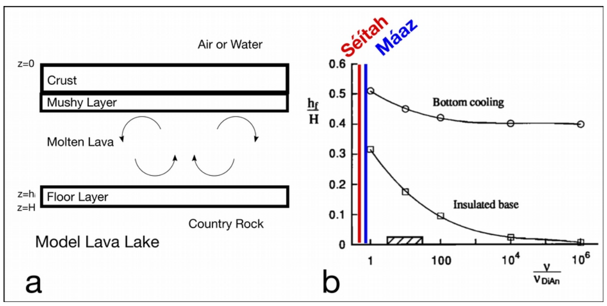

Fig. 4. Thermal model of a lava flow and lava lake. b.) Final fractional height of floor layer, h_f, where crystals accumulate (relative to the height of the chamber height, H) plotted against the lava viscosity (normalized relative to liquid diopside). Two cases are shown, one in which bottom cooling occurs, and one in which it does not (insulated base). The dashed box indicates the viscosity of typical terrestrial basalt relative to a pure diopside melt, after [9]. The Séitah and Máaz viscosities calculated in this paper are schematically shown on the plot.

What have we learned about the Olivine-rich lithology? The olivine-clay-carbonate lithology is among the best-documented rock types in Jezero crater and the surrounding watershed [2-3] and is potentially among the most astrobiologically compelling units in the region [10]. Tying it to the Séitah olivine cumulate is an incomplete task. From orbital VNIR reflectance spectra, the unit contains abundant olivine (Fo#45-66) in large grains (>500 µm, based on band saturation) accompanied by clay and carbonate minerals [4], and its crater retention age is ~3.82 Ga [11]. Several potential origins of the olivine-rich unit are possible: 1) a density segregated melt associated with a lava flow or lake; 2) a pyroclastic density current (PDC) at low temperature [11]; 3) tephra fall [12]; or 4) some combination of all of the above, see also [13]. The transition from primary volcanic deposit to the olivine-clay-carbonate could have been caused by deuteric serpentinization and talc-carbonation [8] perhaps caused by late Noachian CO_2 outgassing [14]. It is also possible that the olivine was altered to carbonate when it was exposed to a thick CO_2-rich Noachian atmosphere [15]. Discrimination between these formation and alteration histories is critical to advancing our understanding of Noachian mantle convective circulation [16].

Why such thin layering and polyhedral jointing? Terrestrial komatiite sequence (usually dunite) lavas have extremely low viscosity, and provide a starting indication for what the lava emplacement mechanism must have been for the olivine-clay-carbonate layers at Seitah and beyond in Nili Fossae. The thin layering (Fig 1) probably also contributes to the draping appearance of the unit reported in [12].

Take away messages: We used CRISM and in-situ data from the Mars2020 rover to examine the properties and emplacement of the olivine-rich lithology. We have found the following:

We find that the viscosity of the Séitah olivine cumulate rock is very low, and flow lengths very long, compared with terrestrial standards.

We have used the SuperCam LIBS instrument to determine Séitah's low (<4wt %) Al_2O_3 - allowing us to eliminate clays with aluminum in their structure.

We hypothesize that the Séitah unit was formed by a ponded lava lake. We also hypothesize that the olivine cumulate was formed at the base of a lava lake within Jezero crater that was part of the region-wide unit.

References: [1] Farley+ (2022) *Science* **377** eabo2196, Liu+ *Science* (2022) 1513-9 Tice+ (2022) *Science Advances* 2375 [2] Ehlmann B.+ (2008) *Science* **322** 1828 [3] Goudge, T.+(2015) *JGR* **120** 775-808 [4] Brown, A.J.+ (2020) *JGR* **125** 2019JE006011; Brown, A.J.+ (2010) *EPSL* **297** 174-182 [5] Giordano+, (2008) *EPSL 271* 123-34 McGetchin and Smythe J.R. (1978) *Icarus* 3 4 512-536 [6] Wiens, R.+ (2022) *Science Advances* **8**, 3399; [7] Beyssace, O.+ (2023) *JGR* Udry, A.+ (20223 *JGR*; Mandon, L.+ (2023) *JGR* [8] Rowland+Harris (2004) *JGR* 109 [9] Worster+ (1993) *JGR* 98. [10] Horgan, B.+ (2020) *Icarus* **339** 113526 [11] Mandon+ (2020) *Icarus* **336** 113436 [12] Kremer, C.+ (2019) *Geology* 111 E02S10 [13] Ravanis, E.+ (2023) LPSC [14] Grott, M.+ *EPSL* **308** 391-400 [15] Pollack, J.B.+ (1987) *Icarus* **71** 203-224 [16] Hirschmann, M.M.+Withers, A.C. *EPSL* **270** 147-155 Kiefer, W.S. (2003) *MAPS* **38** 1815-1832